International Journal of Multimedia and Ubiquitous Engineering
Vol.11, No.3 (2016), pp.115-124
http://dx.doi.org/10.14257/ijmue.2016.11.3.11

Steel Wire Infrared Imagery Defect Detection Based on Gradient Vector Flow Model

Li Li-Jun[1, 2] and Sun Guo-Shuai

1. School of Mechatronic Engineering, China University of Mining and Technology, Xuzhou 221116, China
2. School of Physics Science and Information Engineering, Liaocheng University, Liaocheng 252059, China
E-mail

Abstract

In order to solve the problem regarding steel wire defect detection, a gradient vector flow calculation method based on extended neighborhood is proposed in this article and applied to the steel wire defect detection. The new method is used to analyze the gradient vector flow model from the angle of mask film, wherein the original four- neighborhood mask film is replaced by the mask film with a larger neighborhood, thus to obtain the gradient vector flow calculation method based on the extended neighborhood. Actually, the new calculation method only needs less iterations to obtain better effect. Experimentally, the algorithm proposed in this article is feasible and has high algorithm execution efficiency and high complexity.

Keywords: *Gradient vector flow (GVF); Extended neighborhood; Mask film; Initiative profile model; Steel wire detection*

1. Introduction

Essentially, the initiative profile model aims at defining an initial profile in an image, wherein the initial profile moves towards the target profile direction under the effect of its own internal force and the external force determined by the image in order to automatically converge to the target profile. Specifically, the gradient external force of the edge graph of the image is adopted in the initiative profile model proposed by Kass, *et al*. at the earliest time; the gradient of the edge graph of the image is not equal to zero only at the position with gray level change, namely: the external force is effective only at the image edge, so the external force cannot have any attraction to the curve when the initial profile is located at the position with zero gradient. Therein, GVF obtains its external force field through minimizing an energy functional, and the variational method shall be used during the calculation process to obtain the corresponding Euler equation of the energy functional, and such equation shall be placed in the time evolution framework for iterative solution. During the calculation process, we can find that GVF has strong diffusion effect due to the diffusion effect of Laplace operator and can accordingly form a smooth vector field, wherein we usually adopt four-neighborhood mask film operation to calculate Laplace operator, in other words, only a small part of the image information is adopted during the calculation process. On this basis, a new method is proposed in this article in order to more effectively make use of the image information, and the gradient vector flow based on the extended neighborhood will be extended to a larger neighborhood from the original four-neighborhood Laplace operator, thus to more effectively make use of the image information. Meanwhile, the final experimental result also shows that the new method only needs less iterations to obtain better external force field.

ISSN: 1975-0080 IJMUE

2. Initiative Profile Model and Gradient Vector Flow

The initiative profile model is originally proposed by Kass [1] and essentially aims at defining an initial profile, wherein the initial profile moves towards the target profile under the effect of its own internal force and the external force determined by the image. Additionally, the profile of Snake model is defined by the curve $\mathbf{c}(s)=(x(s),y(s))$ ($s\in[0,1]$) and is namely expressed by the curve with the normalization arc length as the parameter. In Snake model proposed by Kass, the following energy functional is minimized to extract the target profile:

$$E_{snake}=\int_0^1\left[\frac{1}{2}\left(\alpha|c'(s)|^2+\beta|c''(s)|^2\right)+E_{ext}(c)\right]ds \tag{1}$$

Therein, $c'(s)$ and $c''(s)$ respectively refer to the first-order derivative and the second-order derivative of curve $c(s)$ with arc length s as the parameter. In Formula (1), the former two items are the internal energy of the curve. According to relevant curve theory, we can know that the modulus of the first-order derivative denotes the elasticity energy of the curve and can describe the continuity of the curve while the modulus of the second-order derivative denotes the rigidity energy of the curve and can describe the smoothness of the curve.

The smaller the modulus of the first-order derivative, the better the continuity of the curve; the smaller the modulus of the second-order derivative, the better the smoothness of the curve. α and β are the weight parameters, and when α and β are not equal to zero, the curve is a continuous and smooth curve.

$E_{ext}(c)$ refers to the external energy of the curve and is usually constructed according to the feature information of the image, such as gray value and gradient, wherein the external energy is used to attract the initial profile curve to move towards the characteristic direction of the image.

For an image *I* with a given gray level, the typical external energy is determined by the gradient of the image:

$$E_{ext}=-|\nabla I|^2 \text{ or } E_{ext}=-|\nabla G_\sigma\otimes I|^2 \tag{2}$$

Therein, G_σ is a two-dimensional Gaussian function, with the standard deviation as σ.

The variational method is used to solve the minimum value of the energy functional E_{snake}, and Euler equation corresponding to Formula (1) is as follows:

$$-\alpha c''(s)+\beta c''''(s)+\nabla E_{ext}=0 \tag{3}$$

In order to solve the problem existing in original Snake model, Xu and Prince[3] have proposed a new external force field, namely gradient vector flow (GVF) which is used to replace the gradient external force field of the traditional image. Additionally, Xu regards Equation (3) as an internal-external force equilibrium equation:

$$F_{int}+F_{ext}=0 \tag{4}$$

In the above formula, $F_{int}=\alpha c''(s)-\beta c''''(s)$ and $F_{ext}=-\nabla E_{ext}$. Therefore, Xu has proposed a new external force field $\mathbf{v}(x,y)=[u(x,y),v(x,y)]$ and meanwhile minimized the following energy functional to obtain:

$$E_{GVF}=\iint\mu\left(u_x^2+u_y^2+v_x^2+v_y^2\right)+|\nabla f|^2|\mathbf{v}-\nabla f|^2\,dxdy \tag{5}$$

In the above formula: f refers to the edge graph of the image and can be approximated from some edge detection operators or image gradient; μ is the regularization parameter used to adjust the weights of the first item and the second item, wherein the first item is a diffusion item and can be used to diffuse the gradient information of the image to a larger area while the second item is a fidelity term and can protect the edge graph of the image

during the diffusion process. When $|\nabla f|$ is small, the diffusion item plays a leading role in Formula (5) and accordingly generates a slowly changed field; when $|\nabla f|$ is large, the second item plays a leading role therein in order to ensure that the edge is not eliminated during the diffusion process. When $\mu = 0$, GVF field is degraded into a typical image gradient force field; when μ is gradually increased, the smoothness is also gradually increased, thus to enlarge the action range of GVF field and meanwhile eliminate the noise influence more or less.

Based on the variational method, GVF external force field can be obtained through solving the following Euler equation:

$$\begin{aligned} \mu\nabla^2 u - (u - f_x)(f_x^2 + f_y^2) = 0 \\ \mu\nabla^2 v - (v - f_y)(f_x^2 + f_y^2) = 0 \end{aligned} \tag{6}$$

In the above formula, ∇^2 is Laplace operator.

GVF Snake model can well solve such defects of original Snake model as small capture range and initialization sensitivity, and aims at diffusing the gradient vector of the image edge to the surrounding in order to generate a new smooth vector field in the gradient vector field and accordingly enlarge the capture range.

3. Dynamic Gradient Vector Flow Calculation Method Based on Extended Neighborhood

The components of the traditional dynamic GVF along the four directions are understood as the initial iteration solution of GVF external force field $V(x,y) = [u^+(x,y), u^-(x,y), v^+(x,y), v^-(x,y)]$, and $V_t = \mu\nabla^2 \upsilon - (V - df)df^2$ can be regarded as time function, and the steady-state solution can be obtained through partial differential equation $df = [df_x^+, df_x^-, df_y^+, df_y^-]$.

In the above formula,

$$\begin{cases} df_x^+ = \dfrac{\partial}{\partial x} f_x^+ \\ df_x^- = \dfrac{\partial}{\partial x} f_x^- \\ df_y^+ = \dfrac{\partial}{\partial y} f_y^+ \\ df_y^- = \dfrac{\partial}{\partial y} f_y^- \end{cases} \tag{7}$$

$$\begin{cases} \mu^+ = \mu\nabla^2\mu^+ - (\mu^+ - df_x^+)(df_x^+)^2, \mu_0^+ = df_x^+ \\ \mu^- = \mu\nabla^2\mu^- - (\mu^- - df_x^-)(df_x^-)^2, \mu_0^+ = df_x^- \\ \upsilon^+ = \mu\nabla^2\upsilon^+ - (\upsilon^+ - df_y^+)(df_y^+)^2, \upsilon_0^+ = df_y^+ \\ \upsilon^- = \mu\nabla^2\upsilon^- - (\upsilon^- - df_y^-)(df_y^-)^2, \upsilon_0^- = df_y^- \end{cases} \tag{8}$$

$|\nabla f|^2$ is replaced by df^2 in order to decouple $\mu^+, \mu^-, \upsilon^+, \upsilon^-$. Therefore, GVF model is $V_t = g(|\nabla f|)\nabla^2 V - h(|\nabla f|)(V - \nabla f)$, wherein $g(|\nabla f|) = \exp(-\dfrac{|\nabla f|}{K})$ is a monotone decreasing function used to enable the image division edge to have small smoothness but have large diffusion at the position with small edge gradient; $h(|\nabla f|) = 1 - g(|\nabla f|)$ is a

monotone increasing function, and K is used to balance the smoothness and the diffusion. The dynamic GVF vector field is calculated as follows:

$$\varepsilon(V)=\iint[g(|df|)\nabla^2V-h(|df|)](\mu|J_vP|^2)+|V-df|^2]dxdy \tag{9}$$

$$V_t=g(|df|)\nabla^2V-h(|df|)(\mu|J_vP|+V-df) \tag{10}$$

In the above formula, $P=\left[\frac{-g_y}{\sqrt{g_x^2+g_y^2}},\frac{g_y}{\sqrt{g_x^2+g_y^2}}\right]^T$ is defined as the edge pixel position discovery direction and the edge protection energy is accordingly introduced therein; $|J_vP|^2,|J_vP|$ refer to Jacobian determinant and are used to smooth along the edge, without crossing the edge. As a result, the improved GVF fields along various directions can be calculated through iteration according to the above formula.

Through solving Formulae (6) and (9) and placing them in the time framework, the following formula can be obtained:

$$\begin{aligned}\frac{\partial u}{\partial t}&=\mu\nabla^2u-(u-f_x)\left(f_x^2+f_y^2\right)\\ \frac{\partial v}{\partial t}&=\mu\nabla^2v-(v-f_y)\left(f_x^2+f_y^2\right)\end{aligned} \tag{11}$$

The above formula can be further expressed as follows:

$$\begin{aligned}u_t&=\mu\nabla^2u-bu+c_1\\ v_t&=\mu\nabla^2v-bv+c_2\end{aligned} \tag{12}$$

In the above formula, $b=f_x^2+f_y^2$, $c_1=b\cdot f_x$, $c_2=b\cdot f_y$.

f as the edge graph of the image is a constant, so the coefficients b,c_1,c_2 can be calculated in advance and kept unchanged during the whole iteration process. Firstly, $u_t,v_t,\nabla^2u,\nabla^2v$ in Equation (2-12) is discretized to obtain:

$$u_t=\frac{1}{\Delta t}\left(u_{i,j}^{n+1}-u_{i,j}^n\right),\ v_t=\frac{1}{\Delta t}\left(v_{i,j}^{n+1}-v_{i,j}^n\right),$$

$$\nabla^2u=\frac{1}{\Delta x\Delta y}\left(u_{i+1,j}+u_{i-1,j}+u_{i,j+1}+u_{i,j-1}-4u_{i,j}\right),$$

$$\nabla^2v=\frac{1}{\Delta x\Delta y}\left(v_{i+1,j}+v_{i-1,j}+v_{i,j+1}+v_{i,j-1}-4v_{i,j}\right),$$

These discretized formulae are put in Equation (12) to obtain:

$$\begin{aligned}u_{i,j}^{n+1}&=\left(1-b_{i,j}\Delta t\right)u_{i,j}^n+\tau\left(u_{i+1,j}^n+u_{i-1,j}^n+u_{i,j+1}^n+u_{i,j-1}^n-4u_{i,j}^n\right)+c_{1,i,j}\Delta t\\ v_{i,j}^{n+1}&=\left(1-b_{i,j}\Delta t\right)v_{i,j}^n+\tau\left(v_{i+1,j}^n+v_{i-1,j}^n+v_{i,j+1}^n+v_{i,j-1}^n-4v_{i,j}^n\right)+c_{2,i,j}\Delta t\end{aligned} \tag{13}$$

In the above formula, $\tau=\frac{\mu\Delta t}{\Delta x\Delta y}$.

In order to ensure the iteration stability of Equation (13), CFL condition must be met, namely: if $\tau<\frac{1}{4}$ is true, then the condition $\Delta t<\frac{\Delta x\Delta y}{4\mu}$ is met.

The dynamic GVF calculation method based on extended neighborhood is as follows:

$$\varepsilon(V)=\iint[g(|df|)\nabla^2V-h(|df|)](\mu|J_vP|^2)+|V-df|^2]dxdy \tag{14}$$

$$V_t=g(|df|)\nabla^2V-h(|df|)(\mu|J_vP|+V-df) \tag{15}$$

In the above formula, $P=\left[\frac{-g_y}{\sqrt{g_x^2+g_y^2}},\frac{g_y}{\sqrt{g_x^2+g_y^2}}\right]^T$ refers to the normal direction of the edge pixel position and the edge protection energy $\left|J_v P\right|^2$ is accordingly introduced therein, and the dynamic GVF filed based on the extended neighborhood can be calculated through iteration according to Formulae (10) and (11).

According to Formulae (14) and (15), we can find that GVF diffusion is mainly realized through Laplace operator, and the calculation of Laplace operator in the image can be realized by virtue of mask film, wherein the mask film corresponding to Laplace operator is as follows:

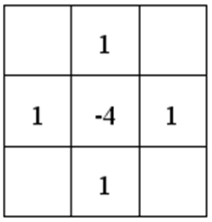

Figure 1. Mask Film Corresponding to Laplace Operator

Mask film operation is frequently used in traditional edge detection. For the traditional edge detection, the detection of brightness discontinuity is usually used to find edges, and the mask film operation for the whole image is most frequently used to find such discontinuity. Meanwhile, the advantage of the application of mask film for calculation lies in the convolution based realization, in other words, convolution operation can be carried out for the image and the corresponding mask film in order to operate all pixels in the image.

According to Figure1, Laplace operator involves in the four-neighborhood mask film operation in the gradient vector flow calculation, so we extend the original four-neighborhood Laplace operator on the basis of the mask film in order to more effectively make use of the image information, as shown in Figure2:

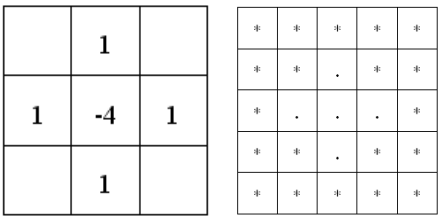

Figure 2. Extension of Laplace Operator to a Larger Neighborhood

Through the extension of Laplace operator to a larger neighborhood, more image information can be used, so we have accordingly proposed the gradient vector flow based on the extended neighborhood. In other words, we adopt the mask film with a larger neighborhood to replace the original four-neighborhood mask film in the calculation of Laplace operator of the gradient vector flow.

We respectively adopt the following mask film operators to calculate the gradient vector flow:

0	0	1	0	0
0	1	1	1	0
1	1	-12	1	1
0	1	1	1	0
0	0	1	0	0

1	1	1	1	1
1	1	1	1	1
1	1	-24	1	1
1	1	1	1	1
1	1	1	1	1

(a) 12-Neighborhood (b) 24-Neighborhood

Figure 3. Extended Neighborhood of Laplace Operator

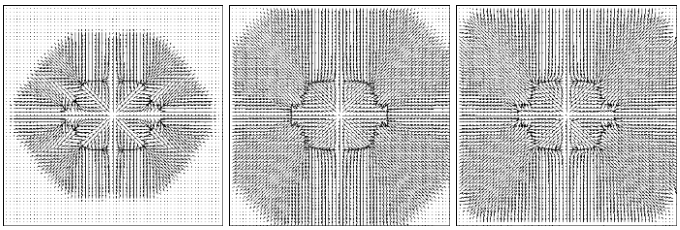

(a) Room Figure (from left to right) 4-Neighborhood GVF, 12-Neighborhood GVF and 24-Neighborhood GVF

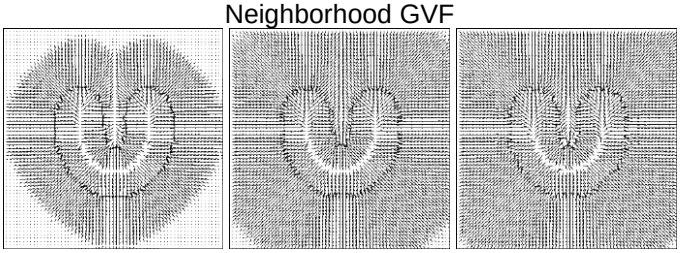

(b) U-Shaped Figure (from left to right) 4-Neighborhood GVF, 12-Neighborhood GVF and 24-Neighborhood GVF

Figure 4. Performance of External Force Field of Gradient Vector Flow Based on Extended Neighborhood (20 Iterations)

4. Experimental Result and Analysis

The vector fields of Room Figure and U-shaped Figure obtained according to Laplace operator based on the extended neighborhood are as shown in Figure4. When calculating the vector field, we execute 20 iterations and find in the experiment: relative to the original gradient vector flow, the dynamic gradient vector flow of Laplace operator based on the extended neighborhood only needs less iterations to obtain large capture range. Meanwhile, such method is applied to actual cardiac images, and the experimental result of the steel wire figure is as shown in Figure5, wherein the iteration time is 20 and Gaussian smoothing parameter is $\sigma = 2.5$. Experimentally, we can know that compared with original gradient vector flow, the gradient vector flow of Laplace operator based on the extended neighborhood needs less iterations.

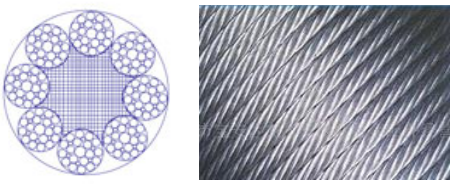

(a) Steel Wire Figure and Edge Graph

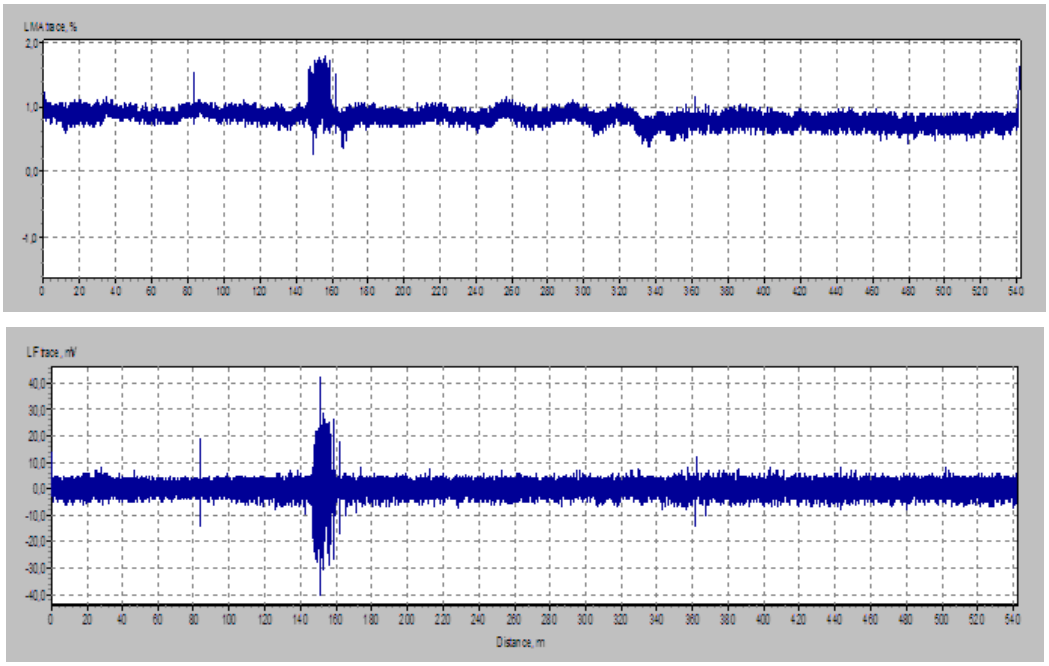

Figure 5. Waveform of Partially Damaged Steel Wire

5. Conclusion

In this article, Laplace operator used in GVF calculation process is analyzed from the angle of image processing mask film and meanwhile the gradient vector flow calculation method based on the extended neighborhood is proposed in order to more effectively make use of the image information. Experimentally, less iterations are needed in the calculation of the gradient vector flow based on the extended neighborhood to obtain relatively smooth vector field. Of course, the gradient vector flow calculation method based on the extended neighborhood also has some defects. For example, the coefficients of the extended neighborhood in the calculation are constants, and the calculation thereof is only simply extended to a larger neighborhood, without the consideration of image structure, so the image structure and the self-adaptive extended neighborhood [11-12] shall be adopted to obtain better effect.

References

[1] J. Hu and Z. Gao, "Distinction immune genes of hepatitis-induced heptatocellular carcinoma", Bioinformatics, vol. 28, no. 24, **(2012)**, pp. 3191-3194.
[2] W. Ke, "Overcoming Hadoop Scaling Limitations through Distributed Task Execution".
[3] Z. Su, X. Zhang and X. Ou, "After we knew it: empirical study and modeling of cost-effectiveness of exploiting prevalent known vulnerabilities across IAAS cloud", Proceedings of the 9th ACM symposium on Information, computer and communications security. ACM, **(2014)**.
[4] G. Bao, L. Mi, Y. Geng and K. Pahlavan, "A computer vision based speed estimation technique for localizing the wireless capsule endoscope inside small intestine", 36th Annual International Conference of the IEEE Engineering in Medicine and Biology Society (EMBC), **(2014)**.

[5] W. Gu, Z. Lv and M. Hao, "Change detection method for remote sensing images based on an improved Markov random field", Multimedia Tools and Applications, **(2016)**.
[6] Z. Lu, C. Esteve, J. Chirivella and P. Gagliardo, "A Game Based Assistive Tool for Rehabilitation of Dysphonic Patients", 3rd International Workshop on Virtual and Augmented Assistive Technology (VAAT) at IEEE Virtual Reality 2015 (VR2015), Arles, France, IEEE, **(2015)**.
[7] Z. Chen, W. Huang and Z. Lv, "Uncorrelated Discriminant Sparse Preserving Projection Based Face Recognition Method", Multimedia Tools and Applications, **(2016)**.
[8] Z. Lv, A. Halawani, S. Feng, H. Li and S. U. Rehman, "Multimodal Hand and Foot Gesture Interaction for Handheld Devices", ACM Transactions on Multimedia Computing, Communications, and Applications (TOMM). 11, 1s, Article 10 **(2014)**, pp. 19.
[9] K. Leng, W. Shi, J. Chen and Z. Lv, "Designing of a I-shaped less-than-truckload cross-dock: A simulation experiments study", International Journal of Bifurcation and Chaos, **(2015)**.
[10] Y. Lin, J. Yang, Z. Lv, W. Wei and H. Song, "A Self-Assessment Stereo Capture Model Applicable to the Internet of Things", Sensors, **(2015)**.
[11] J. He, Y. Geng and K. Pahlavan, "Toward Accurate Human Tracking: Modeling Time-of-Arrival for Wireless Wearable Sensors in Multipath Environment", IEEE Sensor Journal, vol. 14, no. 11, **(2014)**, pp. 3996-4006.
[12] W. Ou, Z. Lv and Z. Xie, "Spatially Regularized Latent topic Model for Simultaneous object discovery and segmentation, "The 2015 IEEE International Conference on Systems, Man, and Cybernetics, **(2015)**.
[13] W. Wang, Z. Lu, X. Li, W. Xu, B. Zhang and X. Zhang, "Virtual Reality Based GIS Analysis Platform. 22th International Conference on Neural Information Processing (ICONIP), Istanbul, Turkey, **(2015)**.
[14] W. Ke, "Using Simulation to Explore Distributed Key-Value Stores for Exascale System Services", 2nd Greater Chicago Area System Research Workshop (GCASR), **(2013)**.
[15] J. He, Y. Geng, F. Liu and C. Xu, "CC-KF: Enhanced TOA Performance in Multipath and NLOS Indoor Extreme Environment", IEEE Sensor Journal, vol. 14, no. 11, **(2014)**, pp. 3766-3774.
[16] S. Zhou, L. Mi, H. Chen and Y. Geng, "Building detection in Digital surface model", 2013 IEEE International Conference on Imaging Systems and Techniques (IST), **(2012)**.
[17] N. Lu, C. Lu, Z. Yang and Y. Geng, "Modeling Framework for Mining Lifecycle Management", Journal of Networks, vol. 9, no. 3, **(2014)**, pp. 719-725.
[18] Y. Geng and K. Pahlavan, "On the accuracy of rf and image processing based hybrid localization for wireless capsule endoscopy", IEEE Wireless Communications and Networking Conference (WCNC), **(2015)**.
[19] G. Liu, Y. Geng and K. Pahlavan, "Effects of calibration RFID tags on performance of inertial navigation in indoor environment", 2015 International Conference on Computing, Networking and Communications (ICNC), **(2015)**.
[20] J. He, Y. Geng, Y. Wan, S. Li and K. Pahlavan, "A cyber physical test-bed for virtualization of RF access environment for body sensor network", IEEE Sensor Journal, vol. 13, no. 10, **(2013)**, pp. 3826-3836.
[21] W. Huang and Y. Geng, "Identification Method of Attack Path Based on Immune Intrusion Detection", Journal of Networks, vol. 9, no. 4, **(2014)**, pp. 964-971.
[22] Y. Su, "In-situ bitmaps generation and efficient data analysis based on bitmaps", In Proceedings of the 24th International Symposium on High-Performance Parallel and Distributed Computing, ACM, **(2015)**, pp. 61-72.
[23] G. Yan, Y. Lv, Q. Wang and Y. Geng, "Routing algorithm based on delay rate in wireless cognitive radio network", Journal of Networks, vol. 9, no. 4, **(2014)**, pp. 948-955.
[24] D. Jiang, X. Ying, Y. Han and Z. Lv, "Collaborative Multi-hop Routing in Cognitive Wireless Networks", Wireless Personal Communications, **(2015)**.
[25] Z. Xiaobing, "Exploring Distributed Resource Allocation Techniques in the SLURM Job Management System", Illinois Institute of Technology, Department of Computer Science, Technical Report, **(2013)**.
[26] G. Bao, L. Mi, Y. Geng, M. Zhou and K. Pahlavan, "A video-based speed estimation technique for localizing the wireless capsule endoscope inside gastrointestinal tract", 2014 36th Annual International Conference of the IEEE Engineering in Medicine and Biology Society (EMBC), **(2014)**.
[27] D. Zeng and Y. Geng, "Content distribution mechanism in mobile P2P network", Journal of Networks, vol. 9, no. 5, **(2014)**, pp. 1229-1236.
[28] L. Tonglin, "ZHT: A light-weight reliable persistent dynamic scalable zero-hop distributed hash table", Parallel & Distributed Processing (IPDPS), 2013 IEEE 27th International Symposium on. IEEE, **(2013)**.
[29] W. Ke, "Optimizing load balancing and data-locality with data-aware scheduling", Big Data (Big Data), 2014 IEEE International Conference on. IEEE, **(2014)**.

Author

Li Lijun, He received his M.S. degree in power electronics and power transmission from Anhui university of Technology in Maanshan, China. He is currently a PhD student in China University of Mining and Technology. His research interest is mainly in the area of non-destructive test. He has published several research papers in scholarly journals in the above research areas.